Journal of the European Ceramic Society 19 (1999) 979–983

PII: S0955-2219(98)00357-4
0955-2219/99/$ - see front matter

Reactive Sintering of Phosphorous Coated $BaTiO_3$

Amador C. Caballero,[a,*] Marina Villegas,[a] José F. Fernández,[a] Carlos Moure,[a] Pedro Durán,[a] Pierre Florian[b] and Jean-Pierre Coutures[b]

[a]Departamento de Electrocerámica, Institute de Cerámica y Vidrio, CSIC, 28500 Arganda del Rey, Madrid, Spain
[b]Centre de Recherche sur la Physique des Hautes Temperatures, 45071 Orleans Cedex, France

Abstract

Doping $BaTiO_3$ with P^{5+} has been reported to decrease the sintering temperature of the ceramic, allowing homogeneous fine grained microstructures to be obtained. According to the present paper, the formation of a phosphorous-BaO rich phase covering the $BaTiO_3$ particles seems to be the origin of the improved porosity coalescence and removal observed at the earlier sintering stage of these materials. The formation and development of phosphorous-barium rich phases have been followed by means of DRX, and high temperature NMR. Phosphorous cations incorporated from phosphate ester form a surface layer covering the $BaTiO_3$ particles which reacts during heating to form $Ba_2TiP_2O_9$ and/or $Ba_3(PO_4)_2$. Formation of these phases seem to occur by solid-solid reaction involving phosphorous diffusion through the $BaTiO_3$ particles. © *1999 Elsevier Science Limited. All rights reserved*

Keywords: phosphate, sintering, microstructure-final, spectroscopy, $BaTiO_3$ and titanates.

1 Introduction

Improved sintering behaviour of $BaTiO_3$ based materials can be achieved by homogeneous doping of the surface of the $BaTiO_3$ particles.[1] For the so called 'grain boundary dopants', this method increases their effectiveness and allows the amount of dopant to be reduced. Both the low concentration and the good distribution of the dopant cations favour their incorporation to the $BaTiO_3$ lattice. Therefore, the presence of secondary phases in the final microstructure can be strongly controlled.

*To whom correspondence should be addressed. Fax: +34-91-870-0550; e-mail: amador@icv.csic.es

Phosphate ester is a dispersant successfully used to prepare tape casting slips,[2] however after the burnt out of the organic chain residual phosphorous remains adsorbed onto the surfaces of the ceramic particles. Phosphate ester addition to PZT, PZT-PNN and Al_2O_3 ceramics has been reported to change their sintering behaviour in a similar way as for $BaTiO_3$.[3–5] For $BaTiO_3$, due to the adsorption characteristics of the phosphate ester,[6] the residual phosphorous forms an homogeneous doping layer covering the $BaTiO_3$ particles. Porosity removal was improved during the first sintering step for this doped material, and the sintering temperature decreased.[5] Taking into account the published data on $BaO–P_2O_5–TiO_2$ and $BaO–P_2O_5$ systems,[7,8] this behaviour could be related to the formation of a reactive layer at temperatures well below the sintering one. In the present work we have studied the nature of the intermediate phases formed during heating in phosphorous-doped $BaTiO_3$ ceramics.

2 Experimental Procedure

The sample preparation process and raw materials properties are reported elsewhere.[5] Assuming that. all the phosphorous present in the phosphate ester remains as P_2O_5, then the P_2O_5 concentration is 5 wt% with respect to the $BaTiO_3$.

The phases present in powders treated at different temperatures for 2 h were determined by powder XRD (X-ray diffraction) and MAS-NMR (Magic Angle Spinning Nuclear Magnetic Resonance). Phases present at high temperature were analyzed in situ by HT-NMR (High Temperature-NMR).

NMR analysis has been carried out in a Bruker DSX 300 spectrometer with a principal field of 7·04 T. The magic angle spinning room temperature solid state ^{31}P NMR spectra were acquired

using a Bruker commercial 4 mm double-bearing MAS probehead. Once the spin-lattice relaxation was estimated for the initial compound, the spectra were then recorded using a pulse excitation of 1·1 μs, where the solution 90° pulse was 9·3 μs, and a recycle delay of 1 s. The cross polarization $\{^1H\text{-}^{31}P\}$ was performed at a spinning speed of 4 kHz with radio-frequency fields of 28 kHz, an optimized contact time of 5 ms. The chemical shifts are referenced to 85% concentrated H_3PO_4 and given ± 0.1 ppm. The chemical shift anisotropy parameters (i.e. isotropic chemical shift, asymmetry parameter and axiality) are extracted from the intensities of the spinning sidebands arising at slow spinning speed (4 kHz), by applying an Herzfeld and Berger procedure.[9]

The high temperature set-up is based on direct irradiation by one CO_2 laser of the sample container placed in the NMR probehead.[10] The sample is placed in a high purity boron nitride crucible, surrounded by a ceramic shield. The radio frequency part of the probehead is cooled to ensure stable irradiation conditions and minimize thermal noise. The temperature is given ± 20°C. The experiments were carried out using a pulse length of 50 μs and a recycle delay of 0.5 s.

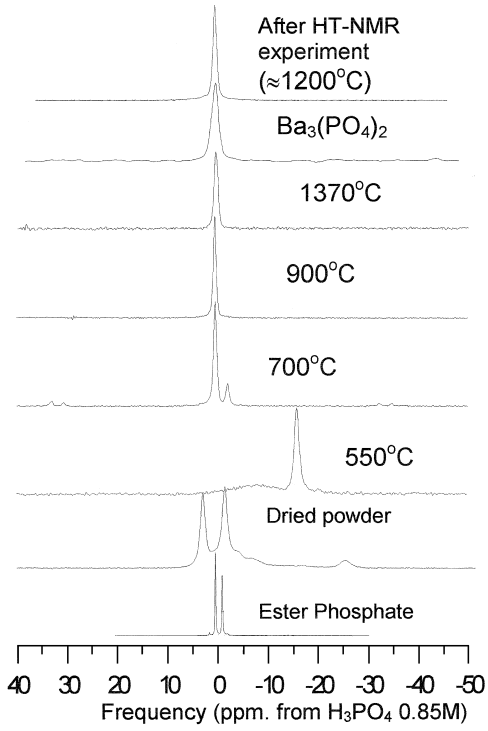

Fig. 1. ^{31}P MAS-NMR spectra for the ester phosphate (60% mono- and 40 di-ester), $Ba_3(PO_2)_2$, dried doped $BaTiO_3$ powder and thermally treated samples.

3 Results and Discussion

3.1 Room temperature analysis

Figure 1 shows the ^{31}P MAS-NMR spectra of ester phosphate (60% mono-and 40 di-ester), $Ba_3(PO_4)_2$, dried doped $BaTiO_3$ powder and thermally treated samples. Table 1 summarises the MAS-NMR results for all the samples analysed. The ester phosphate spectrum shows two main sharp peaks at 0·3 ppm (53%) and $-1{\cdot}1$ ppm (44%) which can be associated to the mono- (60%) and di-ester (40%) molecules, respectively, according to their relative integrated intensities. For the doped dried sample, the spectrum consists of two rather sharp peaks located at 3 and -1 ppm with negative axiality, showing that the phosphorous is in a $Q^{(O)}$ type environment[11] (no P–O–P bonds per PO_4 tetrahedron). The line observed at -1.2 ppm can be attributed to the remaining original di-ester phosphate molecules. However, the other line reflects a totally different phosphorous environment which may be related to the presence of a phosphorous complex

Sample treated at 550°C shows two phosphorous environments. One is characterized by a sharp peak centered at -16 ppm. This corresponds to a $Q^{(O)}$ type phosphorous in a rather ordered phase. This line does not appear under cross-polarization conditions. The second phosphorous site shows a broad line centered at -8 ppm with an axiality of 65 ppm, characteristic of a $Q^{(1)}$ environment in a disordered phase.[11,12] This line shows up under cross-polarization conditions indicating that protons are nearby the phosphorous site. According to reported empirical correlations for the chemical shift value,[12,13] the sharp peak could be associated to $Ti_3(PO_4)_2$. The remaining unreacted phosphorous associated to the broad peak is in a disordered environment which appears after the organic chain of the ester phosphate molecule is burnt out. However DRX analysis of the same sample did not reveal any crystalline phase other than $BaTiO_3$. As it is well known, DRX is more sensitive to the coherent scattering from the grains interior, therefore small amounts of crystalline phases located at the particles surfaces could remain undetected.

Samples treated at 700°C showed two peaks respectively at 0·5 and -2 ppm. The 0·5 ppm resonance line is the main contribution for the samples treated above 700°C. No polarization from protons can be transferred to this line. This corresponds to a $Q^{(O)}$ type of environment free of H^+ and in an ordered phase. The properties and position of this line match both the spectrum observed for the $Ba_3(PO_4)_2$ compound and its reported structure.[14] No polarization from protons can be transferred.to the peak observed at -2 ppm. This is again a $Q^{(0)}$ environment of phosphorous free of H^+. DRX analysis (Fig. 2) revealed the presence of $Ba_3(PO_4)_2$

Table 1. Summary of the measured MAS-NMR spectra

Sample	δ_{ISO}[a]	FWHM[b] ±10Hz	% ±3	Δ_{CSA}[c] ±5ppm	η_{CSA}[d] ±0·2	*CP*[e] *Efficiency*
Ester phosphate	0·3	21	53	N/A	N/A	N/A
	−1·1	23	44	N/A	N/A	N/A
Dried doped powder	2·8	80	36	−60	0·2	+ +
	−1·2	70	29	−65	0·6	+ +
	−3·4	1165	27			+ +
	−22·3	185	8			+ +
Doped 550°C	−7·9	1110	44	65	0·7	+
	−16·4	135	56	−45	0·0	−
Doped 700°C	0·5	795	8			+
	0·5	80	76	−20	0·0	−
	−2	70	16	−45	0·5	−
Doped 900°C	1·7	680	5			+
	0·5	80	95	−20	0·5	−
Doped 1350°C	0·4	85	100	−25	0·0	−
$Ba_3(PO_4)_2$	0·3	65	∼80	−20	0·3	N/A

[a]δ_{ISO}, isotropic chemical shift.
[b]FWHM, full width half maximum.
[c]Δ_{CSA}, axiality parameter.
[d]η_{CSA}, asymetry parameter.
[e]CP, cross-polarization.

(JCPDF #25-0028) and some peaks which could be attributed to $Ba_2TiP_2O_9$ (JCPDF #36-1467).

For the samples treated at 700 and 900°C a small amount of proton containing phase is detected around 1 ppm, however the poor signal-to-noise ratio did not allow to measure the axiality for this compound. XRD of powder sample treated at 900°C showed the presence of three crystalline compounds: $BaTiO_3$, $Ba_3(PO_4)_2$ and $BaTi_4O_9$ (JCPDF #34-0070).

The sample treated at 1370°C showed also the same peak at 0·5 ppm but no other lines were detected under cross polarization conditions. DRX analysis detected three crystalline phases: $BaTiO_3$, $Ba_3(PO_4)_2$ and $BaTi_2O_5$ (JCPDF #34-0133).

3.2 In situ high temperature NMR analysis (static conditions)

Figure 3 shows the ^{31}P NMR spectra of the doped samples at different temperatures. Figure 3(a) shows a first evolution up to 310°C and Fig. 3(b) shows the evolution between 920 and 1190°C. At room temperature the main site in intensity is located around −1 ppm and has a width around 400 Hz, which indicates that it could be the sum of several components. The intensity of the main peak increases up to 150°C approximately due to an increase of the phosphorus mobility reducing the anisotropy of probably all the sites located around 0 ppm. Above this temperature and assuming that no phosphorous is lost at this stage, there is a marked decrease of the phosphorous mobility resulting in a loss of signal intensifies. The initial increase in the phosphorous mobility could be related to the loss of residual water, however when the organic chain starts to decompose the residual

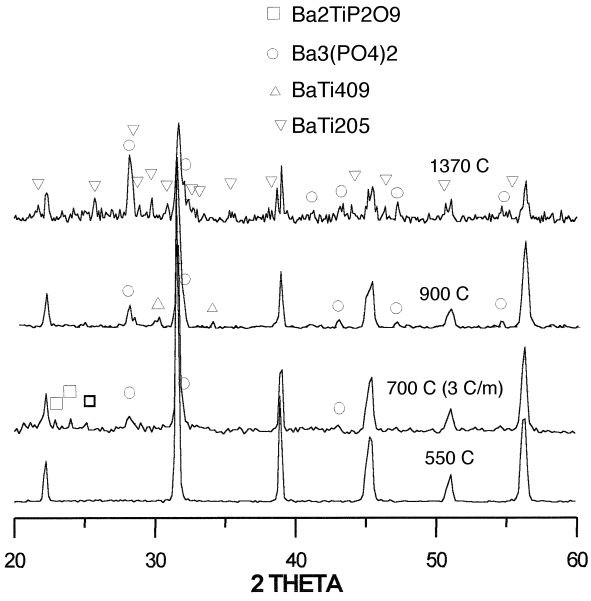

Fig. 2. DRX spectra doped $BaTiO_3$ powder treated at different temperatures. Unmarked peaks (those observed for the sample treated at 550°C) correspond to $BaTiO_3$.

phosphorous cations remain forming a new phase in which they are not allowed to move.

Between 400 and 900°C no phosphorous signal was detected. This indicates that no highly mobile phase is formed, at least in a sufficient amount to be detected by this NMR setup. The crystalline phases observed by DRX in samples treated below 900°C either crystallize during the soaking time and on cooling or the amount and mobility of phosphorous cations initially involved in the reaction is too small to be detected.

A signal is again observed at 920°C [Fig. 3(b)], located at 7 ppm and having a width of 500 Hz. The intensity of the peak increases with temperature pointing out to an increase of the phosphorous

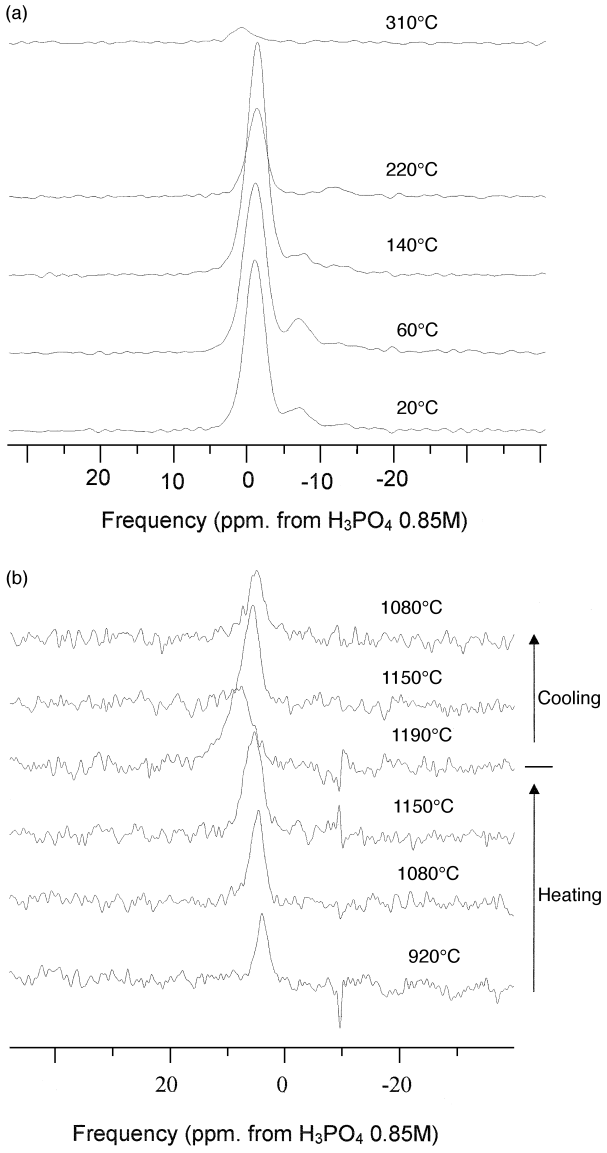

Fig. 3. High temperature ^{31}P NMR spectra of the doped powder: (a) for temperatures below 400°C and (b) for temperatures between 900 and 1200°C.

mobility. On cooling down the chemical shift is recovered, i.e. the composition, however the peak intensity is not fully recovered. Since there is no significant line narrowing compared to the low temperature spectra, the phosphorous observed is not in a low viscosity liquid phase. However at 1190°C the position and width of the peak increase more markedly than for the temperature range 920–1150°C. This could be related to the beginning of melting.

The position of the peak in the high temperature NMR spectra is shifted to higher values than for MAS-NMR spectra and shifts even more when increasing temperature. However, the sample after the high temperature NMR experiment is strictly identical, on ^{31}P NMR point of view, to the powder heat treated at 1370°C (Fig. 1). Therefore, this phase observed *in situ* at high temperature is not $Ba_3(PO_4)_2$ but a different compound which disappears on cooling.

4 Conclusions

Phosphorous cations left by ester phosphate remain as a surface layer covering the $BaTiO_3$ particles. This layer acts as a reactive coating when increasing the temperature. As the temperature increases, a solid state reaction involving phosphorous diffusion through the $BaTiO_3$ particles leads to the formation of a BaO-rich compound at temperatures between 900 and 1200°C. Consequently with the initial phosphorous distribution, this phase is located covering the $BaTiO_3$ particles. Regarding the reported sintering behaviour of P^{5+}-doped $BaTiO_3$, such a layer could act as a diffusion barrier which inhibits mass transport between adjacent grains and favours porosity coalescence and removal at the first stage of sintering. After cooling down, this phase disappears and the crystalline compounds observed are $BaTiO_3$, $Ba_3(PO_4)_2$ and a TiO_2 rich polytitanate.

5 Acknowledgements

The authors would like to thank to CICYT (MAT97-0694-CO2-01) and TMR program 'High and Very High Temperature NMR Spectrometers' ERB FMGE C 950029 for financial support.

References

1. Fernández, J. F., Caballero, A. C., Durán, P. and Moure , C., Improving sintering behaviour of $BaTiO_3$ by small doping additions. *J. Mater. Sci.*, 1996, **31**, 975–981.
2. Mikeska, K. and Cannnon, W. R., Dispersant for tape-casting pure barium titanate. In *Advances in Ceramics, Vol. 9, Forming of Ceramics*, ed. J. A. Mangels, The American Ceramic Society, OH, 1984.
3. Caballero, A. C., Nieto, E., Durán, P., Moure, C., Kosec, M., Samardija, Z. and Drazic, G., Ceramic–electrode interaction in PZT and PNN-PZT multilayer piezoelectric ceramics with Ag/Pd 70/30 inner electrode. *J. Mat. Sci*, 1997, **32**, 3257–3262.
4. Geho, M. and Palmour, H., Sources of sintering inhibition in tape-case aluminas. *Ceram. Eng. Sci. Proc.*, 1993, **14**, 11–12, 97–129.
5. Caballero, A. C., Fernández, J. P., Moure, C. and Durán, P., Effect of residual phosphorous left by phosphate ester on $BaTiO_3$ ceramics. *Mat. Res. Bull*, 1997, **32**(2), 221–229.
6. Le Bars, N, Tinet, D., Faugere, A. M., van Damme, H. and Levitz, P., Adsorption mechanism of phosphate ester on barium titanate in organic medium. Preliminary results on the structure of the adsorbed layer. *J. Phys. III*, 1991, **1**, 707–718.
7. McCauley, R. A. and Hummel, F. A., Phase relationships in a portion of the system $BaO–P_2O_3$. *Trans. Brit. Ceram. Soc.*, 1968, **67**, 619–628.

8. Harrison, D. E., The system $BaO–TiO_2–P_2O_5$: phase relations, fluorescence, and phosphorous preparation. *J. of the Electrochemical Soc.*, 1960, **107**(3), 217–221.
9. Herzfeld, J. and Berger, A. E., Sideband intensities in NMR spectra of samples spinning at the magic angle. *J. Chem. Phys*, 1980, **73**(12), 6021–6029.
10. Brevard, C., Coutures, J. P., Massiot, D., Rifflet, J. C. and Taulle, F., French Pat. FR 8802741.
11. Duncan, T. M. and Douglas, D. C., On the chemical shift anisotropy in condensed phosphate. *Chem. Phys.*, 1984, **87**, 339–349.
12. Turner, G. L., Smith, K. A., Kircpatrick, R. J. and Oldfield, E., Structure and cation effects on phosphorus-31 NMR chemical shifts and chemical shift anisotropies of orthophosphates. *J. of Magn. Reson*, 1986, **70**, 408–415.
13. Losso, P., Schnabel, B., Jäger, C., Sternberg, U., Stachel, D. and Smith, D. O., ^{31}P NMR investigation of binary alkaline earth phosphate glasses of ultra-phosphate composition. *J. Non-Cryst. Solids*, 1992, **143**, 265–273.
14. Zachariasen, W. H., The crystal structure of the normal ortophosphates of barium and strontium. *Acta Cryst.*, 1948, **1**, 263–265.